Journal of Microbiological Methods 246 (2026) 107548

Contents lists available at ScienceDirect

Journal of Microbiological Methods

journal homepage: www.elsevier.com/locate/jmicmeth

Antifungal action of metalated and metal-free porphyrins in the photodynamic inactivation of Sporothrix brasiliensis

Thales Domingos Arantes [a,1,*], Camila Estefany Ribeiro [b], Matheus Fernandes Bezerra de Oliveira [c], Luiz Henrique Barbosa Pires [c], Daniel Graziani [d], Pablo José Gonçalves [e,f,g,1], Guilherme Rocha Lino de Souza [c,h,1]

[a] Centro de Ciências da Saúde, Faculdade de Farmácia, Universidade Federal do Rio Grande do Norte, Rio Grande do Norte, Brazil
[b] Instituto de Patologia Tropical e Saúde Pública, Universidade Federal de Goiás, Goiânia, GO, Brazil
[c] Programa de Pos-graduação em Ciência Animal, Universidade Federal de Goiá, Goiânia, GO, Brazil
[d] Laboratório Multiusuário de Avaliação de Moléculas, Células e Tecidos, Escola de Veterinária e Zootecnia, Universidade Federal de Goiás, Goiânia, GO, Brazil
[e] Instituto de Física, Universidade Federal de Goiás, Goiânia, GO, Brazil
[f] Instituto de Química, Universidade Federal de Goiás, Goiânia, GO, Brazil
[g] Centro de Excelência em Hidrogênio e Tecnologias Energéticas Sustentáveis (CEHTES), Goiânia, GO, Brazil
[h] Instituto de Ciências Biológicas, Universidade Federal de Goiás, Goiânia, GO, Brazil

ARTICLE INFO

Keywords:
Sporothrix brasiliensis
Photoinactivation
Meso-porphyrins
Zinc-meso-porphyrins
Photophysical parameters

ABSTRACT

The thermodimorphic fungi *Sporothrix brasiliensis*, a zoophilic pathogen frequents associated to domestic cats, is the most pathogenic species in *Sporothrix* genus. The increasing resistance of fungal strains to conventional antifungal agents, the prolonged nature and the refractory clinical of treatment underscore the need for alternative therapeutic approaches. Among these, photodynamic inactivation (PDI) has emerged as a promising strategy. PDI involves the combination of a photosensitizing molecule (PS), a light source, and molecular oxygen. Upon irradiation, the PS absorbs photons and undergoes a cascade of photophysical and photochemical reactions that lead to the generation of reactive oxygen species (ROS). At sufficiently high concentrations, these ROS induce irreversible cellular damage, ultimately resulting in cell death. In this study, the *in vitro* photodynamic activity of four porphyrinic photosensitizers against *S. brasiliensis* isolates was evaluated: two cationic porphyrins — *meso*-tetrakis(1-methylpyridinium-4-yl) porphyrin (TMPyP) and its zinc-complexed form (ZnTMPyP) — and two anionic porphyrins — *meso*-tetrakis(4-sulfonatophenyl)porphyrin ($TPPS_4$) and the its zinc-complexed analogue ($ZnTPPS_4$). Fungal susceptibility was determined using the microdilution method in accordance with the Clinical and Laboratory Standards Institute (CLSI) guidelines. Both ZnTMPyP and TMPyP exhibited an estimated minimum effective concentration (MEC) of 0.8 μM against *S. brasiliensis* and *Candida parapsilosis* (control). Among the anionic PSs, $TPPS_4$ showed the greatest inhibitory potential, with an estimated MEC of 1.6 μM. Confocal fluorescence microscopy revealed that both cationic and anionic porphyrins were able to internalize within the cellular structures of *S. brasiliensis*, which may explain the observed inhibitory effects. These findings demonstrate that porphyrin-based PSs, particularly cationic derivatives, effectively inhibit the growth of *S. brasiliensis* isolates. Collectively, the results support the potential application of porphyrins as alternative therapeutic agents for the treatment of sporotrichosis.

1. Introduction

Sporotrichosis is a subcutaneous mycosis with global distribution that primarily affects the skin and subcutaneous tissues of mammals. In immunocompromised individuals, disseminated forms may develop, leading to systemic involvement of bones, lungs, and the central nervous system (Rocha et al., 2024). Pathogens belonging to the *Sporothrix* genus are the etiological agents of this infection, first described in 1898 by Benjamin Schenck (Schenck, 1898). Initially attributed solely to *Sporothrix schenckii*, it is now recognized that *Sporothrix brasiliensis*, *Sporothrix*

* Corresponding author.
E-mail addresses: thales.domingos@ufrn.br (T.D. Arantes), pablo@ufg.br (P.J. Gonçalves), guilherme_lino@ufg.br (G.R.L. de Souza).
[1] Authors contributed equally to this work

https://doi.org/10.1016/j.mimet.2026.107548
Received 26 February 2026; Received in revised form 5 May 2026; Accepted 10 May 2026
Available online 12 May 2026

globosa, and *Sporothrix luriei* also play significant roles in the epidemiology of the disease (Etchecopaz et al., 2020; Rodrigues et al., 2014a).

The species *S. schenckii*, *S. brasiliensis*, *S. globosa*, and *S. luriei* comprise the pathogenic clade responsible for infections in humans and animals, whereas the remaining species form the environmental clade. *S. schenckii* and *S. globosa* have a cosmopolitan distribution and are classically associated with sapronotic transmission through traumatic inoculation of contaminated plant material or organic matter (Gremião et al., 2014). In contrast, *S. brasiliensis* exhibits a distinct epidemiological profile, characterized by predominant enzootic and zoonotic transmission mediated by direct contact with infected cats, including scratches, bites, sneezing, or exudates from lesions (Naliato et al., 2025; Rodrigues et al., 2016). South America reports the highest global prevalence of animal sporotrichosis (81%), and Brazil is considered the epicenter of the epidemic, marked by rapid spread within the feline population and growing public health concern. *S. brasiliensis* is currently the most frequently isolated species, representing approximately 49.92% of reported cases, and until 2014 all confirmed records of this species originated from Brazil (Dumont-Viollaz et al., 2025). Infected cats function as major amplifiers and primary reservoirs of zoonotic transmission, as they commonly develop extensive ulcerative cutaneous lesions with high fungal burden, which may evolve to disseminated disease with multi-organ involvement. This clinical presentation markedly enhances their transmissibility and the likelihood of human infection (Etchecopaz et al., 2021; Conceição, 2026; Barros et al., 2010; Silva et al., 2012).

Currently, the treatment of sporotrichosis in both humans and animals relies on prolonged administration of the fungistatic agent itraconazole (Silva et al., 2012; Rodrigues et al., 2020; Gonçalves et al., 2019). However, this therapy presents several limitations in human treatment, including clinically relevant adverse effects, significant food–drug and drug–drug interactions, high cost, and the need for prolonged treatment courses. In feline cases, an additional concern is the biological risk associated with drug administration. Infected animals often exhibit high fungal burden and extensive cutaneous lesions, which may increase the risk of environmental contamination and zoonotic transmission during handling (Rodrigues et al., 2020; López-Romero et al., 2011; Gremião et al., 2017; Kauffman et al., 2007; Matowane et al., 2018; Tiburcio et al., 2022). Furthermore, the genetic heterogeneity of *Sporothrix* species, combined with incorrect itraconazole use, contributes to the emergence of resistant strains (Waller et al., 2026; Rodrigues et al., 2014b). Therefore, the search for new antifungal agents and bioactive compounds capable of reducing fungal viability and decreasing the fungal burden within lesions, particularly in feline host is essential. Such advances have the potential to shorten treatment duration and accelerate lesion resolution, thereby improving therapeutic outcomes and limiting zoonotic transmission.

In this context, photodynamic inactivation (PDI) has emerged as a promising approach for combating microorganisms and for ectoparasite control (de Freitas et al., 2025; Pires et al., 2025; Moreira et al., 2020; dos Anjos Oliveira et al., 2024; Cocca et al., 2017; Gomes et al., 2024; Chaves et al., 2024; Rapacka-Zdonczyk et al., 2019). Although still in the early stages of application, PDI has demonstrated effectiveness in controlling pathogenic agents associated with sporotrichosis (Rocha et al., 2024; Naliato et al., 2025; Wu and Hu, 2022; Mario et al., 2014). PDI involves the combination of light at a specific wavelength, a photosensitizer (PS), and molecular oxygen, leading to the generation of reactive oxygen species (ROS) such as singlet oxygen and free radicals. These ROS can trigger irreversible oxidative damage to critical biomolecular structures, such as membrane lipids, proteins, carbohydrates, and nucleic acids displayed in several pathogenic agents (de Freitas et al., 2025; Pires et al., 2025; Gomes et al., 2024). In particular, the multitarget oxidative mechanism underlying PDI considerably decreases or even eliminates the likelihood of microbial resistance development, a major limitation in the management of infectious diseases affecting both humans and animals.

Considering the zoonotic emergence of *S. brasiliensis*, the limitations of conventional antifungal therapy, and the therapeutic potential of PDI, the present study investigates porphyrinic photosensitizers with distinct charge profiles, including the cationic *meso*-tetrakis(1-methylpyridinium-4-yl)porphyrin (TMPyP) and its Zn(II) complex (ZnTMPyP), as well as the anionic *meso*-tetrakis(*p*-sulfonatophenyl)porphyrin ($TPPS_4$) and its corresponding Zn(II) complex ($ZnTPPS_4$). These photosensitizers exhibit well-established antimicrobial activity (de Freitas et al., 2025; Teles et al., 2018a; Lopes et al., 2023; Almeida et al., 2012; Merchat et al., 1996), and favorable photophysical properties (Gonçalves et al., 2011; Borissevitch et al., 2023; Mosinger and Micka, 1997), supporting their application in photodynamic protocols. Moreover, it is well established that zinc metalation at the porphyrin core enhances intersystem crossing, leading to increased triplet-state formation and consequently a higher yield of reactive oxygen species. In addition, it improves the hydrophilicity of porphyrins, both features being essential for efficient photodynamic performance (Teles et al., 2018a; Borissevitch et al., 2023; Mosinger and Micka, 1997). By evaluating their performance and investigating their mechanisms of action, this work aims to contribute to the development of alternative strategies for sporotrichosis management in both human and veterinary settings.

2. Methods

2.1. Fungal inocula

Sporothrix brasiliensis isolate used in this study were obtained from the culture collection from LabMicol (Institute of Tropical Pathology and Public Health of the Federal University of Goiás) and maintained in the mycelial phase on Potato Dextrose Agar - PDA (52 $g{\cdot}L^{-1}$) at room temperature. For susceptibility assays, isolates were subcultured on Sabouraud Dextrose Agar - SDA (65 $g{\cdot}L^{-1}$) and incubated at 30 °C for 4–7 days. *C. parapsilosis* (ATCC 22019) was included as a reference control strain. The yeast was maintained through subculturing on Sabouraud Dextrose Agar (65 $g{\cdot}L^{-1}$) and incubated at 35 °C for up to 48 h.

For *S. brasiliensis* mycelial-phase inocula, cultures grown on SDA and after 7 days at 25 °C, colonies were overlaid with 1 mL of sterile saline containing 0.01 mL of tween 20, and conidia were gently released by pipette agitation. The resulting suspension was diluted 1:50 in RPMI-1640 to yield a 2× concentrated stock, corresponding to a final inoculum of approximately 5×10^4 conidia. mL^{-1}.

Yeast inoculum was prepared from culture grown on SDA and incubated at 25–30 °C for 48 h. The small fragments of fungal colonies were suspended in sterile saline (0.85% NaCl) and vortexed until a uniform suspension was obtained. Cell density was adjusted to 0.5 on the McFarland standard scale ($\approx 5 \times 10^6$ cells. mL^{-1}), followed by a 1:50 dilution in RPMI-1640 medium buffered with HEPES.

2.2. Photosensitizers

Photodynamic inactivation of *S. brasiliensis* was carried out using synthetic, water-soluble porphyrins, specifically the anionic *meso*-tetrakis (*p*-sulfonatophenyl) porphyrin ($TPPS_4$), the cationic *meso*-tetrakis (1-methylpyridinium-4-yl) porphyrin (TMPyP), and their respective Zinc(II) complexes ($ZnTPPS_4$ and ZnTMPyP) (Fig. 1). All porphyrins were obtained from Porphyrin Products Inc. (Logan, UT, USA), prepared in phosphate-buffered saline (PBS) and, according to the Lambert-Beer Law, their concentrations were adjusted utilizing the molar absorption coefficients.

2.3. Photophysical parameter measurements

The molar concentrations of the porphyrin samples were determined from their UV–vis absorption spectra according to Beer's law. All measurements were obtained in PBS using a quartz cuvette, and spectra were recorded on a Hitachi U-2900 spectrophotometer.

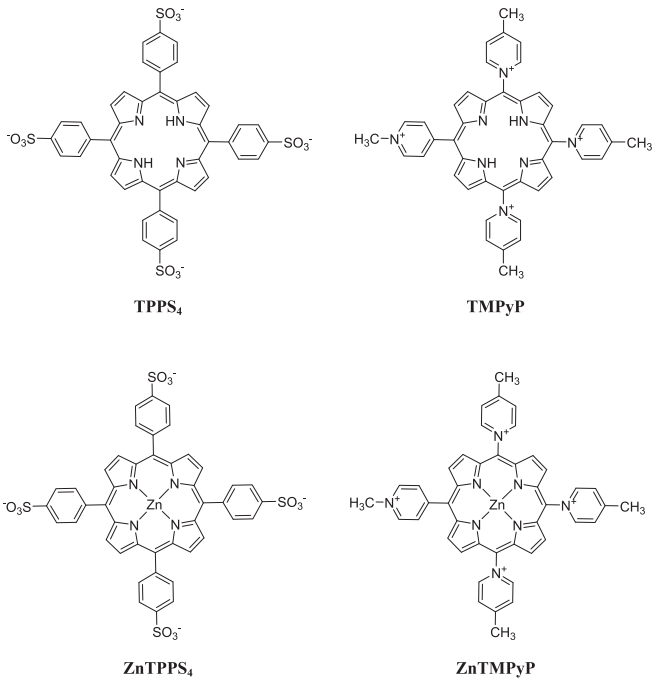

Fig. 1. Molecular structures of porphyrins.

The number of singlet oxygen molecules generated ($n_{1_{O_2}}$) is directly associated with the singlet oxygen quantum yield (Φ_Δ) and with the number of absorbed photons by each photosensitizer (n_{abs}), as described by eq. 1:

$$\Phi_\Delta = \frac{n_{1_{O_2}}}{n_{abs}} \quad (1)$$

The parameter n_{abs} per second can be determined using eq. 2 (de Freitas et al., 2025; Schaberle, 2018):

$$n_{abs} = \int_{\nu_1}^{\nu_2} \frac{P(\nu)}{h\nu}\left(1 - 10^{-A(\nu)}\right)d\nu \quad (2)$$

where h is Planck's constant, ν is the frequency of the incident photons (s^{-1}), $A(\nu)$ represents the absorption spectrum of the photosensitizer, and $P(\nu)$ corresponds to the spectral power distribution of the light source ($W = J.s^{-1}$).

The emission spectrum of the irradiation sources was recorded using an optical fiber coupled to an LSP-2 spectrometer (Laser Line Inc.). The output power was determined with a PM100A power meter equipped with an S470C thermal sensor (Thorlabs). All measurements were performed at controlled room temperature (27 ± 1 °C).

2.4. Antifungal susceptibility testing

Antifungal susceptibility testing was performed to evaluate the response of *S. brasiliensis* to itraconazole, using *Candida parapsilosis* (ATCC 22019) as the reference strain, in accordance with the Clinical and Laboratory Standards Institute (CLSI) guidelines. Yeast and conidia were previously cultured on Sabouraud Dextrose Agar (65 $g{\cdot}L^{-1}$) and incubated at 35 °C for 24–48 h (*C. parapsilosis*) and 96 h (*S. brasiliensis*).

For inoculum preparation, small fragments of yeast colonies were suspended in sterile saline (0.85% NaCl *w/v*) and vortexed until a cell density equivalent to 0.5 on the McFarland turbidity scale was achieved. For conidia preparation, the colonies were washed with sterile saline, and the conidia were separated to prepare the initial dilution. The inoculum was then adjusted to achieve a final concentration of 0.4×10^4 to 5×10^4 CFU/mL, according to the current CLSI M38 guidelines for filamentous fungi. Serial twofold dilutions of itraconazole were prepared in RPMI 1640 medium buffered with HEPES, starting from a stock solution of 16 $\mu g{\cdot}mL^{-1}$ dissolved in dimethyl sulfoxide (DMSO). Equal volumes of the fungal suspension and the drug dilutions were dispensed into 96-well microtiter plates.

Plates were incubated at 35 °C for 24–48 h (*C. parapsilosis*) and 72–96 h (*S. brasiliensis*), and the MIC was determined visually by comparing fungal growth in the control wells. Growth intensity was visually scored on a scale from 0 to 4, where 4 indicated growth equivalent to the positive control and 0 represented complete inhibition of growth (negative control).

2.5. Photodynamic inactivation (PDI) assay

Photodynamic inactivation was evaluated using the broth microdilution method in 96-well plates, adapted from the Clinical and Laboratory Standards Institute (CLSI) guidelines was described for the antifungal tests with itraconazole (CLSI, 2022; CLSI, 2017). Serial twofold dilutions of each photosensitizer (PS) were prepared in 100 µL of RPMI-1640 medium buffered with HEPES, starting from an initial concentration of 3.2 µM. Subsequently, 100 µL of *S. brasiliensis* or *C. parapsilosis* (control) inoculum suspension was added to each well containing the PS solutions and to the positive-control wells.

Plates were incubated at 35 °C for 30 min in the dark. Non-irradiated plates treated with the highest PS concentration (3.2 µM) were included as dark controls to assess intrinsic compound activity. After incubation, samples were irradiated for 30 min using a white LED system (Bio-Lambda®) at an irradiance of 30 mW/cm^2 and a light dose of 108 J/cm^2. To minimize spatial variations in light irradiance across the irradiation field, microplates were centrally positioned within the chamber, excluding approximately 2 cm from the edges, and all experimental conditions were arranged within the central wells. The temperature of the plates was monitored throughout the irradiation process, and a final temperature of approximately 25 °C was recorded, consistent with ambient room conditions.

Plates were subsequently incubated at 35 °C for 48 h for the *C. parapsilosis* control and 96 h for the *S. brasiliensis* (mycelium) isolates, and optical density (OD_{690}) was measured after well homogenization to assess fungal growth. In this study, the minimum effective concentration (MEC) was defined as the lowest photosensitizer concentration that produced the maximum statistically significant inhibition of fungal growth when compared with the untreated control, after correction for background absorbance (PS-only wells).

All assays were performed in duplicate, and data are expressed as mean ± standard deviation. Statistical analysis was performed using one-way ANOVA followed by Tukey's *post hoc* test ($p < 0.05$) in GraphPad Prism® version 6.0.

2.6. Photosensitizer cytolocation assay

Internalization of photosensitizers (PSs) was assessed by confocal fluorescence microscopy, exploiting the intrinsic fluorescence properties of the porphyrins. No additional fluorescent probes or labeling procedures were used. For this analysis, a fungal suspension (150 µL) adjusted to a 0.5 McFarland standard and diluted in sterile saline was incubated with ZnTMPyP or $ZnTPPS_4$ at a final concentration of 50 µM in a microtiter plate. Samples were protected from light and incubated at room temperature for 60 min prior to imaging. Following incubation, the samples were washed three times with sterile saline and centrifuged to remove excess photosensitizer not incorporated into the fungal cells. Approximately 10 µL of the resulting suspension were placed onto a microscope slide, covered with a coverslip, and examined using a confocal fluorescence microscope (TCS SP8 DMi8, Leica Microsystems, Germany) equipped with 10× and 40× objectives. The reaction product generated by the probe was excited with a DPSS 561 laser line at 561 nm, and fluorescence emission was detected at 650 nm. Three-dimensional images were acquired from z-stacks composed of 40

optical sections and reconstructed using Leica LAS X software.

3. Results and discussion

In the context of the increasing global antifungal resistance, along with the limitations and adverse effects associated with conventional therapies, photodynamic inactivation (PDI) has emerged as a promising alternative approach. The present findings indicate that both anionic and cationic photosensitizers exhibit photodynamic activity against *S. brasiliensis* under the tested conditions. These results suggest their potential use as standalone agents or in combination with conventional antifungal therapies. Such combined approaches may improve treatment outcomes in sporotrichosis and other clinically relevant mycoses, including infections by *Candida*, here presented as experimental control isolate. However, further studies are required to confirm these findings and to better establish the role of PDI as a complementary strategy in the management of fungal infections.

3.1. Photophysical characterization and fungal photodynamic inactivation

Fig. 2a displays the absorbed intensity profiles of the porphyrins, calculated as $I_{abs} = 1 - 10^{-A(\lambda)}$, where $A(\lambda)$ represents the wavelength-dependent absorbance. As expected for porphyrinic systems, the spectra are attributed to $\pi \rightarrow \pi^*$ transitions, showing a strong Soret band near 400 nm and a series of weaker Q bands between approximately 470–670 nm. Coordination to Zn(II) produces a noticeable red shift of the Soret band relative to the free-base analogues and leads to the well-known reduction of the Q-band manifold from four transitions to two, consistent with the increased symmetry of the metalated macrocycle (Al-Shewiki et al., 2017).

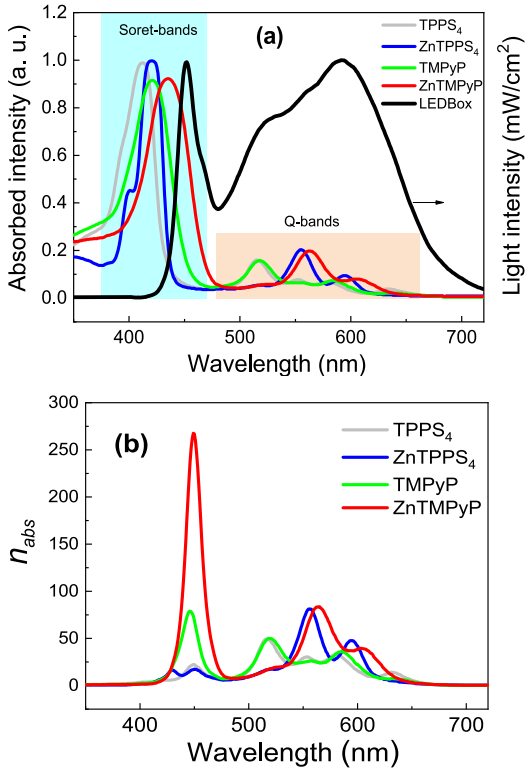

Fig. 2. (a) Absorbed intensity spectra ($I_{abs} = 1 - 10^{-A(\lambda)}$) of the porphyrins $TPPS_4$, $ZnTPPS_4$, TMPP and ZnTMPyP, together with the emission spectrum of the LEDBox light source. (b) Spectra of number of absorbed photons per second (n_{abs}) calculated from the spectral overlap between I_{abs} and the light source power distribution.

The normalized emission spectrum of the LEDBox light source, also shown in Fig. 2a, exhibits substantial spectral overlap with the absorption features of the porphyrins. This overlap indicates that the LEDBox emits appreciable spectral power across the Q-band region and part of the Soret band, reinforcing its suitability as an excitation source for photodynamic applications employing porphyrins as photosensitizers.

The number of absorbed photons per second (n_{abs}) for each porphyrin was calculated by integrating Eq. 2 and is summarized in Table 1. Although the calculations were performed in frequency units, the corresponding n_{abs} spectra are presented as a function of wavelength in Fig. 2b to facilitate direct correlation with the absorption spectra and the power distribution of the light source.

Among the investigated samples, Zn-complexed porphyrins exhibit a higher number of absorbed photons compared to their free-base analogues. According to Eq. 2, n_{abs} is directly associated with the degree of spectral overlap between the emission profile of the irradiation source and the absorption spectrum of the photosensitizer. In this context, the higher n_{abs} values observed for the zinc porphyrins are attributed to enhanced photon absorption in the Q-band region, as can be seen in Fig. 2b. Notably, among the zinc porphyrins, ZnTMPyP exhibits the strongest spectral overlap with the LEDBox emission, particularly within the Soret band region around 450 nm.

The number of singlet oxygen molecules produced ($n_{^1O_2}$) is obtained from the product $n_{abs} \times \Phi_\Delta$, according to Eq. 1, and is presented in Table 1. Again, ZnTMPyP stands out reinforcing its superior efficiency in generating singlet oxygen under LEDBox irradiation.

Among the PSs assessed, the cationic porphyrins ZnTMPyP and TMPyP produced significant inhibition of fungal growth in both *S. brasiliensis* and *C. parapsilosis*, yielding effects significantly compared to the non-treated positive control (Fig. 3).

Considering the anionic photosensitizers, both compounds induced a significant reduction in fungal growth; however, the free-base porphyrin $TPPS_4$ displayed superior activity, of up to 1.6 μM, against *S. brasiliensis* and *C. parapsilosis* when compared with its zinc-coordinated analogue $ZnTPPS_4$ (Fig. 4). As expected, exposure of the model fungus *C. parapsilosis* to the photosensitizers in the absence of light (dark control), even at the highest tested concentrations, resulted in negligible fungicidal activity, confirming that the photosensitizers exhibited no intrinsic toxicity without light activation. This photosafety profile is particularly advantageous for potential topical therapy, wherein localized irradiation of the lesion is required without imposing undue risk of systemic phototoxicity.

The lower MECs obtained for the cationic ZnTMPyP and TMPyP in both fungal species are consistent with the intrinsic photophysical and chemical characteristics of these molecules. In practical terms, some parameters are relevant for the selection of PSs in photodynamic therapy.

Since the photophysical processes in PDI are primarily dependent on photon absorption by the PS, the overlap between the PS absorption bands and the emission spectrum of the irradiation source (LED box) represents a key parameter for PS selection (Fig. 2a). Values of singlet oxygen (ΦΔ) quantum yields, number of photons absorbed (n_{abs}),

Table 1
Values of singlet oxygen (Φ_Δ) quantum yields, number of photons absorbed (n_{abs}), number of singlet oxygen molecules produced ($n_{^1O_2}$) per second for the anionic (TPPS and ZnTPPS) and cationic (TMPyP and ZnTMPyP) porphyrins in PBS.

sample	n_{abs} ($\times 10^{15}$), s^{-1}	Φ_Δ [a,b]	$n_{^1O_2}$ ($\times 10^{15}$), s^{-1} [a,b]	Log $P_{O/W}$ [c]
$TPPS_4$	5.03	0.62	3.12	- 4.0 ± 0.1
$ZnTPPS_4$	5.48	0.74	4.06	- 2.9 ± 0.2
TMPyP	6.93	0.74	5.13	- 3.4 ± 0.1
ZnTMPyP	12.95	0.88	11.40	- 3.0 ± 0.1

a,b and c See refs. (Mosinger and Micka, 1997; Redmond and Gamlin, 1999; Teles et al., 2018b), respectively].

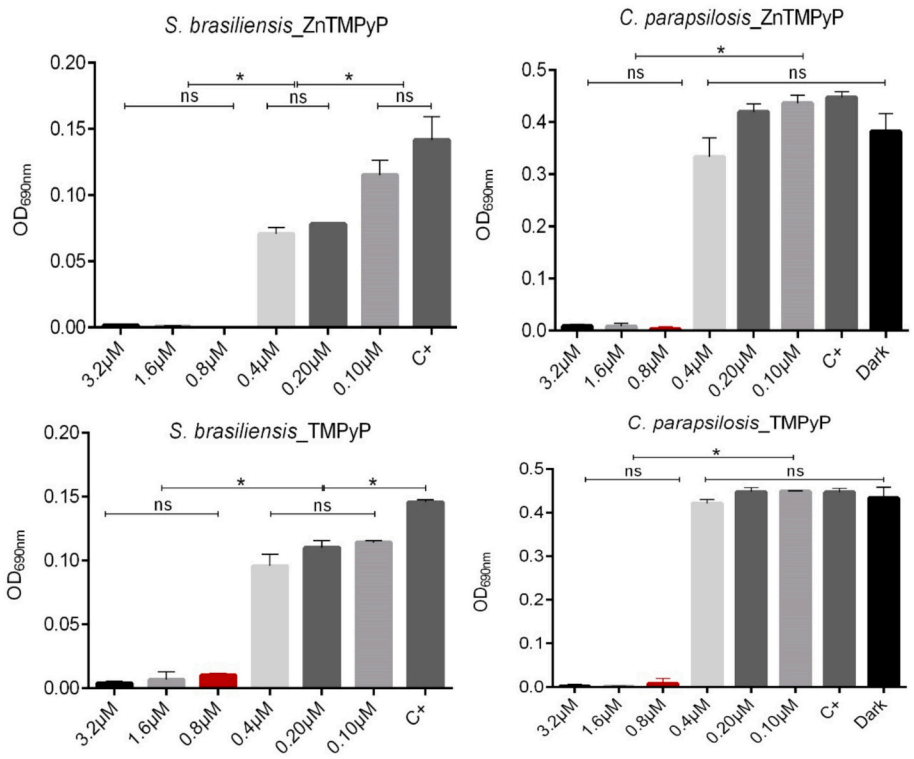

Fig. 3. Photoinactivation of fungal cells (*Sporothrix brasiliensis* and *Candida parapsilosis*) mediated by ZnTMPyP and TMPyP porphyrins following exposure to white LED irradiation. Red bars indicate the MEC determined under the experimental conditions. Statistical analysis was performed using one-way ANOVA followed by Tukey's post-hoc test, where (*) denotes statistically significant differences ($p < 0.05$) and (ns) indicates non-significant differences. (C+) - positive control. (Dark) -dark control. (For interpretation of the references to colour in this figure legend, the reader is referred to the web version of this article.)

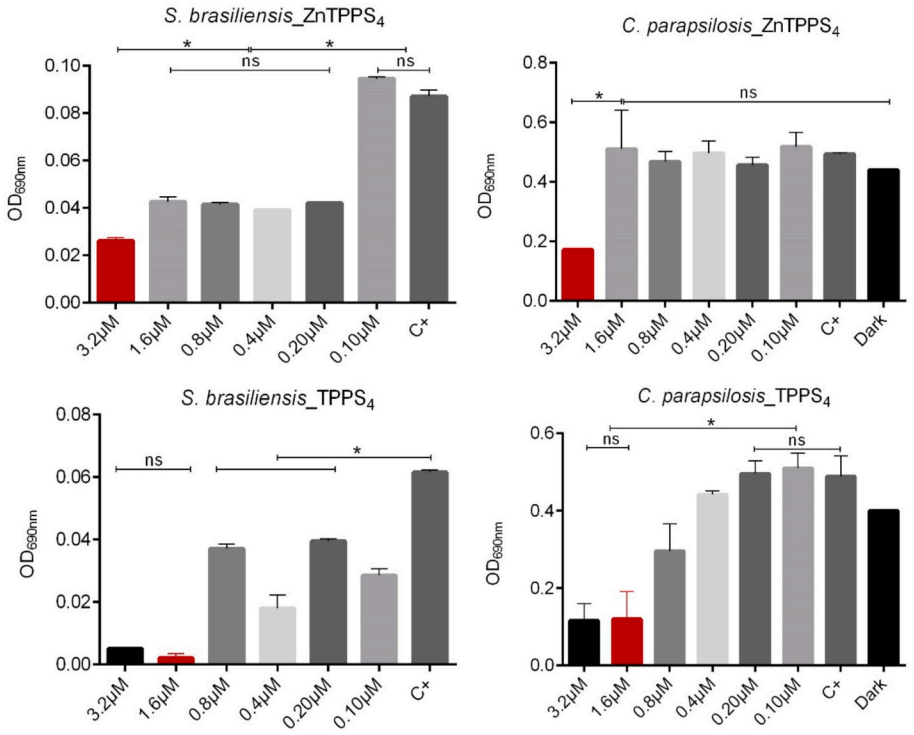

Fig. 4. Photoinactivation of fungal cells (*Sporothrix brasiliensis* and *Candida parapsilosis*) mediated by $ZnTMPPS_4$ and $TPPS_4$ porphyrins following exposure to white LED irradiation. Red bars indicate the MEC determined under the experimental conditions. Statistical analysis was performed using one-way ANOVA followed by Tukey's post-hoc test, where (*) denotes statistically significant differences ($p < 0.05$) and (ns) indicates non-significant differences. (C+) - positive control. (Dark) -dark control. (For interpretation of the references to colour in this figure legend, the reader is referred to the web version of this article.)

number of singlet oxygen molecules produced (n_{1O_2}) per second for metalized porphyrins and their respective free forms are shown in Table 1. Notably, the number of photons absorbed (Fig. 2b) by the ZnTMPyP was significantly higher than that of the other molecules, which likely contributed to the enhancement of the ΦΔ and n_{1O_2} photophysical parameters.

In PDI, singlet oxygen ($^1O_2$) is the most desirable reactive species. The singlet oxygen yields reported for the cationic porphyrins are 88% for ZnTMPyP and 74% for TMPyP, compared to 74% for $ZnTPPS_4$ and 62% for $TPPS_4$ (Table 1), however, these findings alone do not fully account for the superior photodynamic performance of the cationic molecules, as the anionic PSs exhibited comparable singlet oxygen quantum yields despite their reduced antifungal activity.

It is important to note, that singlet oxygen represents only one component of the photophysical processes underlying PDI. Additional reactive oxygen species, such as hydroperoxide, superoxide (O_2^-), hydroxyl radical (OH.) not assessed in the present study, may contribute to the overall photodynamic response and have been implicated in microbial inactivation across diverse systems. However, given that ROS lifetimes are in the nanosecond range (Hatz et al., 2007), higher $^1O_2$ quantum yields are directly associated with greater oxidative damage to biological targets, as observed with ZnTMPyP.

Molecular charges play also a critical role in the interaction of PSs with targets. Considering the cell wall and plasma membrane as the first barrier to PS internalization, cationic PSs display an advantage due to their electrostatic attraction to the negatively charged phospholipid components of biological membranes. Such interactions likely promote enhanced cellular uptake. Once internalized, or even when associated with the membrane, the PS can interact with a wide range of biological targets through oxidative mechanisms.

Also relates to the charges, the presence or absence of polar groups in the PS molecular structure contribute to its solubility. Analysis of the partition coefficients (Log $P_{O/W}$) indicates that both cationic and anionic photosensitizers exhibit substantial hydrophilicity (Table 1). Although the presence of zinc atom into the porphyrin core has been reported to further decrease hydrophilicity (Wilkinson et al., 1993), his behavior did not interfere with the cellular internalization of PSs in the structures of *S. brasiliensis*, as observed in images obtained from confocal fluorescence microscopy assay (Fig. 6).

Given the still incipient number of studies exploring photodynamic inactivation for the treatment of sporotrichosis, the findings presented in this work gain particular importance from a public health perspective. Among the photosensitizers reported in the specialized literature, methylene blue (MB) stands out as the most frequently employed compound, showing significant antifungal activity both *in vitro* and in experimental animal models (Mario et al., 2014; Li et al., 2019). Clinical trials using MB in patients diagnosed with sporotrichosis have also demonstrated improvement of fungal lesions on the skin (García-Malinis et al., 2018; Gilaberte et al., 2014) and in the oral cavity (da Silva et al., 2024a). Cabral et al. (2022) further reported a case of complete clinical remission following treatment with 0.01% MB gel-PDI combined with oral itraconazole, after two sessions of red laser irradiation (Cabral et al., 2022).

In veterinary medicine, cats represent the most affected species and the main vector of sporotrichosis transmission (De Andrade Galliano Daros Bastos et al., 2025). Due to its favorable cost-benefit ratio, MB is often adopted in photodynamic therapy protocols for feline sporotrichosis. However, earlier studies have described methylene blue as toxic to cats, and its use has been contraindicated in many cases owing to adverse effects such as hemolytic anemia, Heinz body formation and renal failure (da Silva et al., 2024b; Schechter et al., n.d.).

Considering new-generation molecules, a recent *in vitro* study employing the RuPDIp complex as a photosensitizer against *S. brasiliensis* and *C. albicans*, a total reduction of fungal growth was achieved at a concentration of 0.5 μM at 525 nm using a light dose of 25.2 J/cm^2 (Tiburcio et al., 2022). In a subsequent work, the same research group evaluated curcumin mediated PDI of *Sporothrix spp.* and demonstrated that, although several studies support the feasibility of PDI for controlling sporotrichosis, none of the photosensitizers tested, except the RuPDIp complex, produced a higher reduction in fungal growth compared with curcumin (Tiburcio et al., 2022).

In accordance with these previous findings, our results show that for the photosensitizers ZnTMPyP, TMPyP, and $TPPS_4$, a MIC of 0.8 μM, for the cationic PSs, were sufficient to completely inhibit fungal growth in both *S. brasiliensis* and *C. parapsilosis*.

Moreover, although most of the absorption spectrum of porphyrins lies below 600 nm, a slight overlap between the porphyrin absorption and the emission spectrum of the radiation source is observed within the well known therapeutic window (>600 nm), especially in the more shifted Q bands (~620–650 nm). Considering that sporotrichosis lesions may extend beyond superficial regions of the skin (Orofino-Costa et al., 2022; de Lima Barros et al., 2011), this overlap could still promote deeper light penetration into the lower layers of the irradiated tissue, thereby enhancing the photodynamic action against fungal cells located in deeper strata. However, the extent to which this contributes to therapeutic efficacy requires further investigation under *in vivo* conditions (Gao et al., 2022; Correia et al., 2021; da Silva et al., 2025).

The mycelial form of *S. brasiliensis* was selected for the screening and characterization of photosensitizers due this morphological phase presents a greater number of natural barriers, including a well-organized cell wall and melanin deposition, which are known to confer enhanced resistance to antifungal agents (Waller et al., 2026; Romero et al., 2023; Almeida-Paes et al., 2016; Gómez-Gaviria et al., 2023; Sanchotene et al., 2017). Under this approach, the photosensitizers identified and the minimum effective concentrations established in this study are also expected to be sufficient for the photodynamic inactivation of infective yeast form of the fungus. In fact, a comparative study on the photodynamic action of photosensitizers against different morphological phases of *S. brasiliensis* revealed that its yeast form is as susceptible to photodamage as the mycelial phase at the same RuPDIp complex concentration (Tiburcio et al., 2022). Therefore, it is reasonable to assume that the minimal effective concentrations determined in the present study may also be suitable for the photodynamic inactivation of sporotrichosis in its infective yeast form.

3.2. Susceptibility profile to antifungal agent

Although the *S. brasiliensis* strain used in this study was originally isolated from a feline source, it did not exhibit resistance to itraconazole when compared to the reference strain *Candida parapsilosis* (Fig. 5). While similar MEC values were observed for itraconazole (0.71 μM) and the tested photosensitizers (0.8 μM), it is important to note that these approaches are based on fundamentally different mechanisms of action and experimental conditions. Therefore, direct comparisons between antifungal susceptibility assays and photodynamic inactivation should be interpreted with caution, especially when observing the possible differences between the mycelial (tested) and yeast-like phases of *S. brasiliensis*. In this context, the results suggest that photodynamic inactivation may represent a complementary strategy to conventional antifungal therapy, rather than a direct alternative.

Due to the broad range of cellular targets affected by photosensitizers, the risk of resistance development or selection is significantly reduced, or even absent, when compared to standard antifungal agents. Moreover, PDT offers versatile therapeutic applications, as activation of

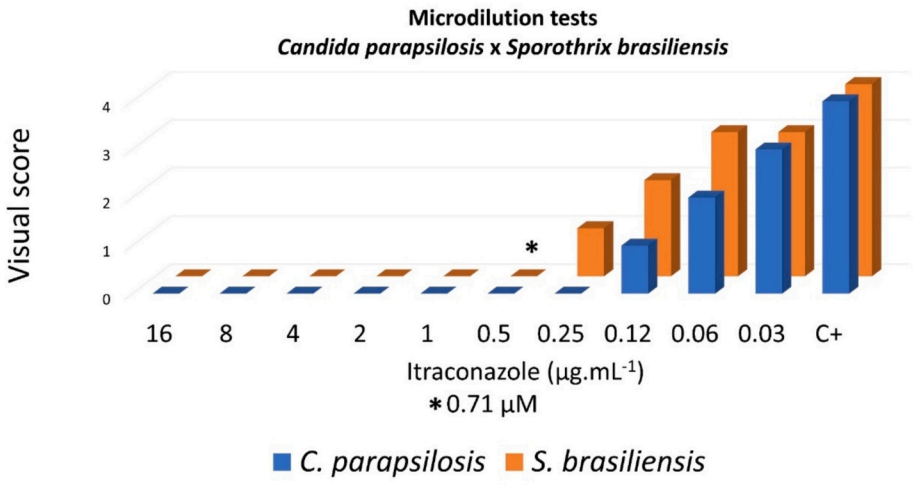

Fig. 5. Comparative antifungal susceptibility testing of *S. brasiliensis* and *C. parapsilosis*. *Minimum effective concentration (MEC) of 0.5 µg/mL for *S. brasiliensis*, corresponding to 0.71 µM of itraconazole.

the photosensitizers is restricted to the irradiated area, allowing their use in both topical and systemic approaches, particularly for localized lesions.

Although the present study did not specifically investigate combinatorial strategies, the potential for synergy between photosensitizers and antifungal agents remains an important consideration. Previous studies have demonstrated successful outcomes using methylene blue in combination with itraconazole in feline photodynamic therapy (Cabral et al., 2022), supporting the relevance of this approach.

ROS produced during PDI are highly reactive and non-selective, targeting a broad range of cellular biomolecules including lipids, proteins, nucleic acids, and carbohydrates. This broad-spectrum mechanism may account for the less sharply defined dose-response curves typically observed in PDI compared with those from itraconazole susceptibility assays. In PDI, a rapid collapse in fungal growth is often detected at the MEC, likely due to the simultaneous oxidative damage to multiple cellular components. This extensive damage may exceed the fungal antioxidant defense capacity, leading to irreversible cellular disruption and rapid cell death.

The use of *Candida parapsilosis* as a reference strain should be interpreted with caution, as differences in morphology and physiology between yeast and filamentous fungi may limit direct comparisons. The inclusion of a *Sporothrix* reference strain, such as *Sporothrix schenckii* ATCC 10268, would provide a more appropriate benchmark for future studies.

A limitation of our study in clinical correlations is the use of the mycelial phase of *S. brasiliensis*, whereas the yeast form is the clinically relevant morphology associated with parasitic phase and zoonotic transmission. Therefore, the present findings should be interpreted as a preliminary *in vitro* assessment, with association with saprophyte phase (mycelial phase) to infection process. Additionally, although the assays were performed at 35 °C to approximate physiological conditions to parasitic phase (also indicate at CLSI protocol), this temperature may not be optimal for filamentous growth, which typically occurs at lower temperatures. Further studies evaluating the yeast phase under appropriate conditions are necessary to confirm the applicability of these results in parasitic phase.

It is important to note that antifungal susceptibility profiles obtained *in vitro* may not fully reflect *in vivo* efficacy, as host factors such as immune response, tissue environment, and pharmacokinetics can significantly influence treatment outcomes (Bidaud et al., 2021). Therefore, the present findings should be considered as a preliminary assessment, and further studies, including *in vivo* models, are required to validate the therapeutic potential of these photosensitizers.

3.3. Distribution of photosensitizers across fungal morphological structures

Metalated photosensitizers (PSs) were preferentially selected for internalization assays in *S. brasiliensis* due to their superior photophysical properties, particularly their enhanced ability to generate reactive oxygen species. Confocal fluorescence microscopy indicated the internalization of these metalated PSs, as fluorescence signals were observed within fungal cellular compartments. Although fluorescence intensity was not quantitatively measured, the microscopy images suggested intracellular localization of the photosensitizers in hyphae, indicating their ability to cross the cell wall and plasma membrane (Fig. 6, yellow arrows). In contrast, fluorescence emission appeared weaker in conidia. This reduced signal may be associated with the higher melanin content in conidial cell walls (Nosanchuk et al., 2015; Staats et al., 2013; Vicentefranqueira et al., 2018; Moreno et al., 2007), which can absorb excitation light and attenuate fluorescence emission from these structures (Fig. 6, white arrows). Overall, these observations qualitatively support the occurrence of photosensitizer uptake under the experimental conditions. However, as no quantitative uptake analysis was performed, the relationship between intracellular accumulation and photodynamic efficacy cannot be fully established and should be interpreted with caution.

Regarding the internalization process, gene expression regulation in *S. brasiliensis*, as in most fungi, involves zinc finger domain-containing proteins (ZFPs). For instance, the zinc-responsive transcription factor ZafA (orthologous to *S. cerevisiae* Zap1) regulates zinc uptake transporters under zinc-limited conditions, thereby influencing cellular zinc homeostasis (Staats et al., 2013; Vicentefranqueira et al., 2018; Moreno et al., 2007; Tangsombatvichit et al., 2015). This regulatory network may affect the uptake of zinc-based photosensitizers. Therefore, the presence of zinc ions in both cationic (ZnTMPyP) and anionic ($ZnTPPS_4$) complexes may contribute to their internalization. Once internalized, irradiated PSs trigger a cascade of photodynamic reactions. These may proceed *via* type I mechanisms, generating ROS such as superoxide anions ($\bullet O_2^-$), peroxides (O_2^{2-}), and hydroxyl radicals ($\bullet OH$), or *via* type II mechanisms, which predominantly produce singlet oxygen ($^1O_2$), the key cytotoxic species in PDI (Baptista et al., 2017; Jablonski, 1933).

Although the internalization assays were conducted only with metalated photosensitizers, the relatively low molecular mass and high aqueous solubility of all compounds suggest that other PSs may also penetrate fungal structures. This property may contribute to the photodynamic activity observed in the PDI assays, although with different levels of efficacy among the tested compounds.

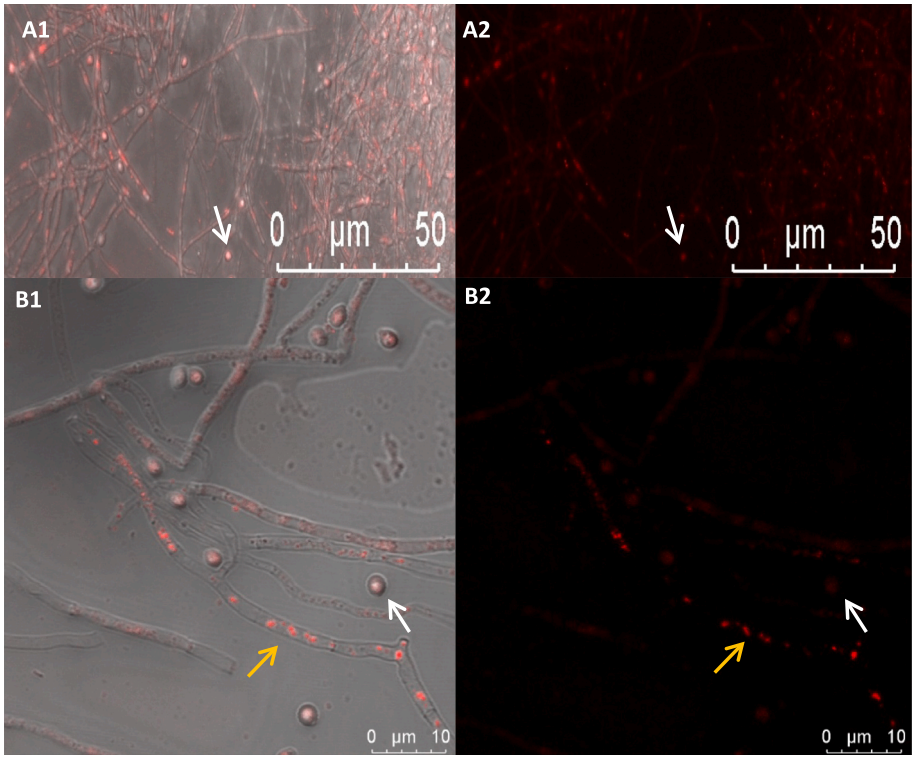

Fig. 6. Distribution of porphyrin-associated fluorescence within *S. brasiliensis* cell structures. The filamentous morphology of the fungus exhibits characteristic hyphae (indicated by yellow arrows) and conidia (indicated by white arrows). Panels A1/A2 and B1/B2 correspond to cellular uptake of ZnTMPyP and $ZnTPPS_4$ porphyrins, respectively. (For interpretation of the references to colour in this figure legend, the reader is referred to the web version of this article.)

4. Conclusion

The cationic porphyrins ZnTMPyP and TMPyP exhibited superior efficacy in the photodynamic inactivation of *Sporothrix brasiliensis* and *Candida parapsilosis* compared with the anionic porphyrins ZnTPPS and TPPS. However, given the low MEC values obtained (0.8–1.6 µM), it is plausible that higher concentrations of the anionic porphyrins could further improve their photodynamic performance. The photophysical parameters were consistent with the superior activity of ZnTMPyP, which displayed a considerably higher number of absorbed photons than the other photosensitizers when irradiated with LED system at an irradiance of 30 mW/cm^2 and a light dose of 108 J/cm^2, indicating its strong potential for clinical application.

Despite the advantage of ZnTMPyP, the anionic porphyrin ZnTPPS also demonstrated efficient internalization in both hyphae and conidia, suggesting that optimized concentration adjustments could enhance the performance of both photosensitizers. According to our findings, and considering the growing global resistance to conventional antifungal agents and their associated toxicity, the photosensitizers evaluated in this study may represent potential candidates for the photodynamic control of *S. brasiliensis*. In sporotrichosis, where lesions may harbor high fungal loads, reducing fungal burden and promoting lesion resolution are important for improving clinical outcomes. In this context, photodynamic inactivation could potentially contribute to shortening the duration of active infection, which may indirectly reduce the risk of zoonotic transmission. However, this hypothesis requires further investigation.

CRediT authorship contribution statement

Thales Domingos Arantes: Writing – original draft, Supervision, Resources, Methodology, Investigation, Funding acquisition, Conceptualization. **Camila Estefany Ribeiro:** Methodology, Investigation. **Matheus Fernandes Bezerra de Oliveira:** Methodology, Investigation. **Luiz Henrique Barbosa Pires:** Writing – original draft. **Daniel Graziani:** Methodology. **Pablo José Gonçalves:** Writing – original draft, Supervision, Resources, Investigation, Funding acquisition, Conceptualization. **Guilherme Rocha Lino de Souza:** Writing – original draft, Supervision, Resources, Methodology, Investigation, Funding acquisition, Formal analysis, Conceptualization.

Acknowledgements and funding

The authors gratefully acknowledge financial support from: National Council for Scientific and Technological Development (CNPq), with grant no. 409486/2018-3, 302390/2023-5, 142162/2025-6 and 406572/2025-9; National Institute of Science and Technology in Innovative Research in Health Sciences from Nanotechnology to Artificial Intelligence (INCT PICS) sponsored by Brazil's National Council for Scientific and Technological Development (CNPq), grant no. 408417/2024-2; Coordination of Superior Level Staff Improvement (Capes), grant no. 88887.197686/2025-00; São Paulo Research Foundation (FAPESP), grant no. 2025/26818-7; and Goiás State Research Support Foundation (FAPEG), grant no. 202310267000475, 202310267001300, 202310267001362 and 202310267000218.

Declaration of competing interest

The authors declare that they have no known competing financial interests or personal relationships that could have appeared to influence the work reported in this paper.

Data availability

No data was used for the research described in the article.

References

Almeida, L.M., Zanoelo, F.F., Castro, K.P., Borissevitch, I.E., Soares, C.M.A., Gonçalves, P.J., 2012. Cell survival and altered gene expression following photodynamic inactivation of paracoccidioides brasiliensis. Photochem. Photobiol. 992–1000. https://doi.org/10.1111/j.1751-1097.2012.01112.x.

Almeida-Paes, R., Figueiredo-Carvalho, M.H.G., Brito-Santos, F., Almeida-Silva, F., Oliveira, M.M.E., Zancopé-Oliveira, R.M., 2016. Melanins protect Sporothrix brasiliensis and Sporothrix schenckii from the antifungal effects of terbinafine. PLoS One 11. https://doi.org/10.1371/journal.pone.0152796.

Al-Shewiki, R.K., Mende, C., Buschbeck, R., Siles, P.F., Schmidt, O.G., Rüffer, T., Lang, H., 2017. Synthesis, spectroscopic characterization and thermogravimetric analysis of two series of substituted (metallo)tetraphenylporphyrins. Beilstein J. Nanotechnol. 8, 1191–1204. https://doi.org/10.3762/bjnano.8.121.

Baptista, M.S., Cadet, J., Di Mascio, P., Ghogare, A.A., Greer, A., Hamblin, M.R., Lorente, C., Nunez, S.C., Ribeiro, M.S., Thomas, A.H., Vignoni, M., Yoshimura, T.M., 2017. Type I and type II photosensitized oxidation reactions: guidelines and mechanistic pathways. Photochem. Photobiol. 93, 912–919. https://doi.org/10.1111/php.12716.

Bidaud, A.L., Schwarz, P., Herbreteau, G., Dannaoui, E., 2021 Feb 4. Techniques for the assessment of in vitro and in vivo antifungal combinations. J Fungi (Basel). 7 (2), 113. https://doi.org/10.3390/jof7020113. PMID: 33557026; PMCID: PMC7913650.

Borissevitch, I.E., Silveira-Alves, E., Almeida, C.G.L., Souza, G.R.L., Sokolov, S.S., Gonçalves, P.J., 2023. An alternative method to determine the quantum yield of the excited triplet state using laser flash photolysis. Photonics 10. https://doi.org/10.3390/photonics10040409.

Cabral, F.V., Sellera, F.P., Ribeiro, M.S., 2022. Feline sporotrichosis successfully treated with methylene blue-mediated antimicrobial photodynamic therapy and low doses of itraconazole. Photodiagn. Photodyn. Ther. 40. https://doi.org/10.1016/j.pdpdt.2022.103154.

Chaves, I., Morais, F.M.P., Vieira, C., Bartolomeu, M., Faustino, M.A.F., Neves, M.G.P.M.S., Almeida, A., Moura, N.M.M., 2024. Can porphyrin-Triphenylphosphonium conjugates enhance the photosensitizer performance toward bacterial strains? ACS Appl. Bio Mater. 7, 5541–5552. https://doi.org/10.1021/acsabm.4c00659.

CLSI, 2017. Reference method for broth dilution antifungal susceptibility testing of filamentous fungi, 3rd ed. CLSI standard M38, Wayne, PA.

CLSI, 2022. Performance standards for antifungal susceptibility testing of filamentous fungi, 3rd ed. CLSI supplement M61, Wayne, PA.

Cocca, L.H.Z., Oliveira, T.M.A., Gotardo, F., Teles, A.V., Menegatti, R., Siqueira, J.P., Mendonça, C.R., Bataus, L.A.M., Ribeiro, A.O., Souza, T.F.M., Souza, G.R.L., Gonçalves, P.J., De Boni, L., 2017. Tetracarboxy-phthalocyanines: from excited state dynamics to photodynamic inactivation against bovine herpesvirus type 1. J. Photochem. Photobiol. B 175, 1–8. https://doi.org/10.1016/j.jphotobiol.2017.08.019.

Barros, MBL, Schubach, TP, Coll, JO, Gremião, ID, Wanke, B, Schubach, A, 2010. Esporotricose: a evolução e os desafios de uma epidemia. Rev. Panam. Salud Publica. 27 (6), 455–460. https://doi.org/10.1590/S1020-49892010000600009.

Bastos de Lima Barros, M. nica, Schubach, A. de Oliveira, Francesconi do Valle, A. nio Carlos, Gutierrez Galhardo, M. Clara, Conceiçã o-Silva, F. tima, Pacheco Schubach, T. nia Maria, Reis, R. Santos, Wanke, B., Feldman Marzochi, K. Belizia, Conceição, M. José, 2026. Cat-Transmitted Sporotrichosis Epidemic in Rio de Janeiro, Brazil: Description of a Series of Cases. https://academic.oup.com/cid/article/38/4/529/352030.

Correia, J.H., Rodrigues, J.A., Pimenta, S., Dong, T., Yang, Z., 2021. Photodynamic therapy review: principles, photosensitizers, applications, and future directions. Pharmaceutics 13. https://doi.org/10.3390/pharmaceutics13091332.

da Silva, W.R., da Costa Almeida, M.V., Gominho, L., Albuquerque, A.C.M.M., Cavalcanti, U.D.N.T., de F.S. Cavalcanti, L., Romeiro, K., 2024a. Photodynamic therapy in the coadjuvant treatment of *Sporothrix schenckii* complex. Spec. Care Dentist. 44, 486–490. https://doi.org/10.1111/scd.12904.

da Silva, W.R., da Costa Almeida, M.V., Gominho, L., Albuquerque, A.C.M.M., Cavalcanti, U.D.N.T., de F.S. Cavalcanti, L., Romeiro, K., 2024b. Photodynamic therapy in the coadjuvant treatment of *Sporothrix schenckii* complex. Spec. Care Dentist. 44, 486–490. https://doi.org/10.1111/scd.12904.

da Silva, L.B.B., Castilho, I.G., de Souza Silva, F.A., Ghannoum, M., Garcia, M.T., do Carmo, P.H.F., 2025. Antimicrobial photodynamic therapy for superficial, skin, and mucosal fungal infections: An update. Microorganisms 13. https://doi.org/10.3390/microorganisms13061406.

De Andrade Galliano Daros Bastos, F., De Farias, M.R., Gremião, I.D.F., Bridi Cavassin, F., Dos Santos Monti, F., Vilas Boas, R.R., Lustosa, B.P.R., Razzolini, E., Vicente, V.A., Queiroz-Telles, F., 2025. Cat-transmitted sporotrichosis by <italic>Sporothrix brasiliensis</italic>: focus on its potential transmission routes and epidemiological profile. Med. Mycol. 63. https://doi.org/10.1093/mmy/myaf051.

de Freitas, A.B., Rezende, H.H.A., de Souza, G.R.L., Gonçalves, P.J., 2025. Photodynamic inactivation of KPC-producing Klebsiella pneumoniae difficult-to-treat resistance (DTR) by a cationic porphyrin. J. Photochem. Photobiol. B 265. https://doi.org/10.1016/j.jphotobiol.2025.113133.

de Lima Barros, M.B., de Almeida Paes, R., Schubach, A.O., 2011. Sporothrix schenckii and sporotrichosis. Clin. Microbiol. Rev. 24, 354–633. https://doi.org/10.1128/CMR.00007-11.

dos Anjos Oliveira, T.M., Teles, A.V., Gambarini, M.L., de Oliveira Ribeiro, K., Ducas, E.S.A., dos Santos, K.J.G., Monteiro, C.J.P., de Paula Silveira Lacerda, E., Franchi, L.P., Gonçalves, P.J., de Souza, G.R.L., 2024. Photodisinfection of *Alphaherpesvirus* 1 in bovine semen. J. Photochem. Photobiol. B 260. https://doi.org/10.1016/j.jphotobiol.2024.113036.

Dumont-Viollaz, A., dos Santos, A.R., Thomson, P., 2025. Zoonotic sporotrichosis: systematic review and clinical aspects of feline and canine cases. Med. Mycol. 63. https://doi.org/10.1093/mmy/myaf060.

Etchecopaz, A.N., Lanza, N., Toscanini, M.A., Devoto, T.B., Pola, S.J., Daneri, G.L., Iovannitti, C.A., Cuestas, M.L., 2020. Sporotrichosis caused by Sporothrix brasiliensis in Argentina: case report, molecular identification and in vitro susceptibility pattern to antifungal drugs. J. Mycol. Médicale 30. https://doi.org/10.1016/j.mycmed.2019.100908.

Etchecopaz, A., Toscanini, M.A., Gisbert, A., Mas, J., Scarpa, M., Iovannitti, C.A., Bendezú, K., Nusblat, A.D., Iachini, R., Cuestas, M.L., 2021. Sporothrix brasiliensis: A review of an emerging south american fungal pathogen, its related disease, presentation and spread in Argentina. Journal of Fungi 7, 1–33. https://doi.org/10.3390/jof7030170.

Gao, J., Chen, Z., Li, X., Yang, M., Lv, J., Li, H., Yuan, Z., 2022. Chemiluminescence in combination with organic photosensitizers: beyond the light penetration depth limit of photodynamic therapy. Int. J. Mol. Sci. 23. https://doi.org/10.3390/ijms232012556.

García-Malinis, A.J., Milagro Beamonte, A., Torres Sopena, L., García-Callen, O., Puertolas-Villacampa, P., Gilaberte, Y., 2018. Cutaneous sporotrichosis treated with methylene blue-daylight photodynamic therapy. J. Eur. Acad. Dermatol. Venereol. 32, e90–e91. https://doi.org/10.1111/jdv.14545.

Gilaberte, Y., Aspiroz, C., Alejandre, M. Carmen, Andres-Ciriano, E., Fortuño, B., Charlez, L., Revillo, M.J., Hamblin, M.R., Rezusta, A., 2014. Cutaneous sporotrichosis treated with photodynamic therapy: an in vitro and in vivo study. Photomed. Laser Surg. 32, 54–57. https://doi.org/10.1089/pho.2013.3590.

Gomes, I.C.P., Divino, L.D.A., Rodrigues, F.M., Fleury, C.M.F., Ducas, E.S.A., Desordi, J. C., Iglesias, B.A., Santana, R.C., Monteiro, C.M.O., Lopes, W.D.Z., Gonçalves, P.J., Souza, G.R.L., 2024. Daylight photodynamic inactivation of cattle tick Rhipicephalus microplus by porphyrins: An alternative for the ectoparasite control. J. Photochem. Photobiol. B 251. https://doi.org/10.1016/j.jphotobiol.2024.112847.

Gómez-Gaviria, M., Martínez-Álvarez, J.A., Mora-Montes, H.M., 2023. Current Progress in Sporothrix brasiliensis basic aspects. Journal of Fungi 9. https://doi.org/10.3390/jof9050533.

Gonçalves, P.J., Franzen, P.L., Correa, D.S., Almeida, L.M., Takara, M., Ito, A.S., Zílio, S. C., Borissevitch, I.E., 2011. Effects of environment on the photophysical characteristics of mesotetrakis methylpyridiniumyl porphyrin (TMPyP). Spectrochim. Acta A Mol. Biomol. Spectrosc. 79, 1532–1539. https://doi.org/10.1016/j.saa.2011.05.012.

Gonçalves, J., Gremião, I., Kölling, G., Duval, A., Ribeiro, P., 2019. Esporotricose, o gato e a comunidade. Enciclopédia Biosfera 16, 769–787. https://doi.org/10.18677/encibio_2019a62.

Gremião, I.D.F., Menezes, R.C., Schubach, T.M.P., Figueiredo, A.B.F., Cavalcanti, M.C.H., Pereira, S.A., 2014. Feline sporotrichosis: epidemiological and clinical aspects. Med. Mycol. 53, 15–21. https://doi.org/10.1093/mmy/myu061.

Gremião, I.D.F., Miranda, L.H.M., Reis, E.G., Rodrigues, A.M., Pereira, S.A., 2017. Zoonotic epidemic of Sporotrichosis: cat to human transmission. PLoS Pathog. 13. https://doi.org/10.1371/journal.ppat.1006077.

Hatz, S., Lambert, J.D.C., Ogilby, P.R., 2007. Measuring the lifetime of singlet oxygen in a single cell: addressing the issue of cell viability. Photochem. Photobiol. Sci. 6, 1106–1116. https://doi.org/10.1039/b707313e.

Jablonski, A., 1933. Efficiency of anti-stokes fluorescence in dyes. Nature 131, 839–840. https://doi.org/10.1038/131839b0.

Kauffman, C.A., Bustamante, B., Chapman, S.W., Pappas, P.G., 2007. Clinical practice guidelines for the management of sporotrichosis: 2007 update by the infectious diseases society of america. Clin. Infect. Dis. 45, 1255–1265. https://doi.org/10.1086/522765.

Li, J., Zhu, M., An, L., Chen, F., Zhang, X., 2019. Fungicidal efficacy of photodynamic therapy using methylene blue against Sporothrix globosa in vivo and in vivo. Eur. J. Dermatol. 29, 160–166. https://doi.org/10.1684/ejd.2019.3527.

Lopes, P., Joaquinito, A.S.M., Ribeiro, A., Moura, N.M.M., Gomes, A.T.P., Guerreiro, S.G., Faustino, M.A.F., Almeida, A., Ferreira, P., Coimbra, M.A., Neves, M.G.P.M.S., Gonçalves, I., 2023. Starch-based films doped with porphyrinoid photosensitizers for active skin wound healing. Carbohydr. Polym. 313. https://doi.org/10.1016/j.carbpol.2023.120894.

López-Romero, E., Reyes-Montes, M.D.R., Pérez-Torres, A., Ruiz-Baca, E., Villagómez-Castro, J.C., Mora-Montes, H.M., Flores-Carreón, A., Toriello, C., 2011. Sporothrix schenckii complex and sporotrichosis, an emerging health problem. Future Microbiol. 6, 85–102. https://doi.org/10.2217/fmb.10.157.

Mario, D.A.N., Denardi, L.B., Pereira, D.I.B., Santurio, J.M., Alves, S.H., 2014. In vitro photodynamic inactivation of *Sporothrix schenckii* complex species. Med. Mycol. 52, 770–773. https://doi.org/10.1093/mmy/myu041.

Matowane, R.G., Wieteska, L., Bamal, H.D., Kgosiemang, I.K.R., Van Wyk, M., Manume, N.A., Abdalla, S.M.H., Mashele, S.S., Gront, D., Syed, K., 2018. In silico analysis of cytochrome P450 monooxygenases in chronic granulomatous infectious fungus *Sporothrix schenckii*: special focus on CYP51. Biochim. Biophy. Acta Proteins Proteomics 1866, 166–177. https://doi.org/10.1016/j.bbapap.2017.10.003.

Moreira, X., Santos, P., Faustino, M.A.F., Raposo, M.M.M., Costa, S.P.G., Moura, N.M.M., Gomes, A.T.P.C., Almeida, A., Neves, M.G.P.M.S., 2020. An insight into the synthesis of cationic porphyrin-imidazole derivatives and their photodynamic inactivation efficiency against Escherichia coli. Dyes Pigments 178. https://doi.org/10.1016/j.dyepig.2020.108330.

Moreno, M.Á., Ibrahim-Granet, O., Vicentefranqueira, R., Amich, J., Ave, P., Leal, F., Latgé, J.P., Calera, J.A., 2007. The regulation of zinc homeostasis by the ZafA transcriptional activator is essential for aspergillus fumigatus virulence. Mol. Microbiol. 64, 1182–1197. https://doi.org/10.1111/j.1365-2958.2007.05726.x.

Mosinger, J, Micka, Z, 1997. Quantum yields of singlet oxygen of metal complexes of meso-tetrakis(sulphonatophenyl) porphine. J. Photochem. Photobiol. A Chem. 107 (1–3), 77–82. https://doi.org/10.1016/S1010-6030(96)04613-8.

Naliato, G.F.S., Arantes, T.D., Rodrigues, A.M., Pimentel de Barros, P., Castanho Scortecci, K., Fernanda França, G., da Silva Cordeiro, M.L., Theodoro, R.C., 2025. Virulence assessment of *Sporothrix* species from clinical and environmental clades using *Tenebrio molitor* as an experimental model. Med. Mycol. 63. https://doi.org/10.1093/mmy/myaf092.

Nosanchuk, J.D., Stark, R.E., Casadevall, A., 2015. Fungal melanin: what do we know about structure? Front. Microbiol. 6. https://doi.org/10.3389/fmicb.2015.01463.

Orofino-Costa, R., Freitas, D.F.S., Bernardes-Engemann, A.R., Rodrigues, A.M., Talhari, C., Ferraz, C.E., Veasey, J.V., Quintella, L., de Sousa, M.S.L.A., Vettorato, R., de Almeida-Paes, R., de Macedo, P.M., 2022. Human sporotrichosis: recommendations from the Brazilian Society of Dermatology for the clinical, diagnostic and therapeutic management. An. Bras. Dermatol. 97, 757–777. https://doi.org/10.1016/j.abd.2022.07.001.

Pires, L.H.B., dos Anjos Oliveira, T.M., Desordi, J.C., Ducas, E.S.A., Souza, L.S., de Moraes, E.C., Borsanelli, A.C., Batista, A.A., Gonçalves, P.J., de Souza, G.R.L., 2025. Breaking antibiotic resistance: porphyrin-driven photoinactivation and priming effect on mastitis-related MDR bacteria. J. Photochem. Photobiol. B 271. https://doi.org/10.1016/j.jphotobiol.2025.113246.

Rapacka-Zdonczyk, A., Wozniak, A., Pieranski, M., Woziwodzka, A., Bielawski, K.P., Grinholc, M., 2019. Development of Staphylococcus aureus tolerance to antimicrobial photodynamic inactivation and antimicrobial blue light upon sub-lethal treatment. Sci. Rep. 9. https://doi.org/10.1038/s41598-019-45962-x.

Redmond, R.W., Gamlin, J.N., 1999. A compilation of singlet oxygen yields from biologically relevant molecules. Photochem. Photobiol. 70, 391–475. https://doi.org/10.1111/j.1751-1097.1999.tb08240.x.

Merchat, M, Bertolini, G, Giacomini, P, Villanueva, A, Jori, G, 1996. Meso-substituted cationic porphyrins as efficient photosensitizers of gram-positive and gram-negative bacteria. J. Photochem. Photobiol. B. 32 (3), 153–157. https://doi.org/10.1016/1011-1344(95)07147-4. PMID: 8622178.

A.R. Rocha, N.M. Inada, A.P. da Silva, V.S. Bagnato, H.H. Buzzá, Photodynamic inactivation strategies for maximizing antifungal effect against *Sporothrix* spp. and *Candida albicans* in an in vitro investigation, PLoS Negl. Trop. Dis. 2024-November (2024). doi:https://doi.org/10.1371/journal.pntd.0012637.

Rodrigues, A.M., De Hoog, G., Zhang, Y., De Camargo, Z.P., 2014a. Emerging sporotrichosis is driven by clonal and recombinant sporothrix species. Emerg. Microbes Infect. 3. https://doi.org/10.1038/emi.2014.33.

Rodrigues, A.M., de Hoog, G.S., de Cássia Pires, D., Brihante, R.S.N., da Costa Sidrim, J. J., Gadelha, M.F., Colombo, A.L., De Camargo, Z.P., 2014b. Genetic diversity and antifungal susceptibility profiles in causative agents of sporotrichosis. BMC Infect. Dis. 14. https://doi.org/10.1186/1471-2334-14-219.

Rodrigues, A.M., de Hoog, G.S., de Camargo, Z.P., 2016. *Sporothrix* species causing outbreaks in animals and humans driven by animal–animal transmission. PLoS Pathog. 12. https://doi.org/10.1371/journal.ppat.1005638.

Rodrigues, A.M., Della Terra, P.P., Gremião, I.D., Pereira, S.A., Orofino-Costa, R., de Camargo, Z.P., 2020. The threat of emerging and re-emerging pathogenic Sporothrix species. Mycopathologia 185, 813–842. https://doi.org/10.1007/s11046-020-00425-0.

Romero, V., Kalinhoff, C., Saa, L.R., Sánchez, A., 2023. Fungi's Swiss Army knife: pleiotropic effect of melanin in fungal pathogenesis during cattle mycosis. Journal of Fungi 9. https://doi.org/10.3390/jof9090929.

Sanchotene, K.O., Brandolt, T.M., Klafke, G.B., Poester, V.R., Xavier, M.O., 2017. In vitro susceptibility of Sporothrix brasiliensis: comparison of yeast and mycelial phases. Med. Mycol. 55, 869–876. https://doi.org/10.1093/mmy/myw143.

Schaberle, F.A., 2018. Assessment of the actual light dose in photodynamic therapy. Photodiagn. Photodyn. Ther. 23, 75–77. https://doi.org/10.1016/j.pdpdt.2018.06.009.

R.D. Schechter, O.W. Schalm, J.J. Kaneko, Heinz Body Hemolytic Anemia Associated with the Use of Urinary Antiseptics Containing Methylene Blue in the Cat, n.d.

Schenck, B.R., 1898. On refractory subcutaneous abscesses caused by a fungus possibly related to the sporotricha.

Silva, MBT, Costa, MMM, Torres, CCS, Galhardo, MCG, Valle, ACF, Magalhães, MAFM, et al., 2012. Esporotricose urbana: epidemia negligenciada no Rio de Janeiro. Brasil. Cad Saúde Pública. 28 (10), 1867–1880. https://doi.org/10.1590/S0102-311X2012001000006.

Staats, C.C., Kmetzsch, L., Schrank, A., Vainstein, M.H., 2013. Fungal zinc metabolism and its connections to virulence. Front. Cell. Infect. Microbiol. 4. https://doi.org/10.3389/fcimb.2013.00065.

Tangsombatvichit, P., Semkiv, M.V., Sibirny, A.A., Jensen, L.T., Ratanakhanokchai, K., Soontorngun, N., 2015. Zinc cluster protein Znf1, a novel transcription factor of non-fermentative metabolism in Saccharomyces cerevisiae. FEMS Yeast Res. 15. https://doi.org/10.1093/femsyr/fou002.

Teles, A.V., Oliveira, T.M.A., Bezerra, F.C., Alonso, L., Alonso, A., Borissevitch, I.E., Gonçalves, P.J., Souza, G.R.L., 2018a. Photodynamic inactivation of bovine herpesvirus type 1 (Bohv-1) by porphyrins. J. Gen. Virol. 99, 1301–1306. https://doi.org/10.1099/jgv.0.001121.

Teles, A.V., Oliveira, T.M.A., Bezerra, F.C., Alonso, L., Alonso, A., Borissevitch, I.E., Gonçalves, P.J., Souza, G.R.L., 2018b. Photodynamic inactivation of bovine herpesvirus type 1 (BoHV-1) by porphyrins. J. Gen. Virol. 99, 1301–1306. https://doi.org/10.1099/jgv.0.001121.

Tiburcio, M.A., Rocha, A.R., Romano, R.A., Inada, N.M., Bagnato, V.S., Carlos, R.M., Buzzá, H.H., 2022. In vitro evaluation of the cis-[Ru(phen)2(pPDIp)]2+** complex for antimicrobial photodynamic therapy against Sporothrix brasiliensis and Candida albicans. J. Photochem. Photobiol. B 229. https://doi.org/10.1016/j.jphotobiol.2022.112414.

Vicentefranqueira, R., Amich, J., Marín, L., Sánchez, C.I., Leal, F., Calera, J.A., 2018. The transcription factor ZafA regulates the homeostatic and adaptive response to zinc starvation in aspergillus fumigatus. Genes (Basel) 9. https://doi.org/10.3390/genes9070318.

Waller, S.B., Flores, D., Lana, D., Quatrin, P.M., Roberto, M., Ferreira, A., Alexandre, Fuentefria, M., Mezzari, A., 2026. Antifungal resistance on *Sporothrix* species: an overview. Clin. Microbiol. Rev. https://doi.org/10.1007/s42770-020-00307-z/Published.

Wilkinson, F., Helman, W.P., Ross, A.B., 1993. Quantum yields for the photosensitized formation of the lowest electronically excited singlet state of molecular oxygen in solution. J. Phys. Chem. Ref. Data Monogr. 22, 113–262. https://doi.org/10.1063/1.555934.

Wu, X., Hu, Y., 2022. Photodynamic therapy for the treatment of fungal infections. Infect. Drug Resist. 15, 3251–3266. https://doi.org/10.2147/IDR.S369605.